**Hydrology and Earth System Sciences**

Discussions

Open Access

# Use of field and laboratory methods for estimating unsaturated hydraulic properties under different land-use

S. Siltecho[1,4,5], C. Hammecker[2], V. Sriboonlue[3,4], C. Clermont-Dauphin[2], V. Trelo-ges[1,4], A. C. D. Antonino[6], and R. Angulo-Jaramillo[7]

[1]Department of Plant Science and Land Resource, Faculty of Agriculture, Khon Kaen University, Thailand
[2]Institut de Recherche pour le Développement (IRD), UMR 210, place Viala, Montpellier, France
[3]Department of Agricultural Engineering, Faculty of Engineering, Khon Kaen University, Thailand
[4]Ground Water Research Center, Khon Kaen University, Thailand
[5]Land Development Regional Office No. 5, Land Development Department, Ministry of Agriculture, Thailand
[6]Universiadade Federal do Pernambuco, Centro de Tecnologia, Departamento de Energia Nuclear, Recife, Brazil
[7]Univserité de Lyon, UMR5023 Ecologie des Hydrosystèmes Naturels et Anthropisés, Université Lyon 1, ENTPE, CNRS, 3, rue Maurice Audin, 69518 Vaulx-en-Velin, France

Discussion Paper | Discussion Paper | Discussion Paper | Discussion Paper |

HESSD

11, 6099–6137, 2014

**Estimating unsaturated hydraulic properties**

S. Siltecho et al.

Title Page

Abstract | Introduction

Conclusions | References

Tables | Figures

|◄ | ►|

◄ | ►

Back | Close

Full Screen / Esc

Printer-friendly Version

Interactive Discussion

**Estimating unsaturated hydraulic properties**

S. Siltecho et al.

Title Page

Abstract | Introduction

Conclusions | References

Tables | Figures

Back | Close

Full Screen / Esc

Printer-friendly Version

Interactive Discussion

Discussion Paper | Discussion Paper | Discussion Paper | Discussion Paper

## Abstract

Adequate water management is required to improve the efficiency and sustainability of agricultural systems when water is scarce or over-abundant, especially in the case of land-use changes. In order to quantify, to predict and eventually to control water and solute transport into soil, soil hydraulic properties need to be determined precisely. As their determination is often tedious, expensive and time-consuming, many alternative field and laboratory techniques are now available. The aim of this study was to determine unsaturated soil hydraulic properties under different land-uses and to compare the results obtained with different measurement methods (Beerkan, Disk infiltrometer, Evaporation, pedotransfer function). The study has been realised on a tropical sandy soil in a mini watershed in NE Thailand. The experimental plots were positioned in a rubber tree plantation in different positions along a slope, in ruzi grass pasture and in an original forest site. Non parametric statistics demonstrated that van Genuchten unsaturated soil parameters ($K_s$, $\alpha$ and $n$), were significantly different according to the measurement methods employed whereas location was not a significant discriminating factor when all methods were considered together. However within each method, parameters $n$ and $\alpha$ were statistically different according to the sites. These parameters were used with Hydrus1D for a one year simulation and computed pressure head did not show noticeable differences for the various sets of parameters, highlighting the fact that for modelling, any of these measurement method could be employed. The choice of the measurement method would therefore be motivated by the simplicity, robustness and its low cost.

## 1 Introduction

Rubber tree (*Hevea brasiliensis*) has become a crop of high economic interest in the Northeast of Thailand since the price raise of natural rubber on the international market and the policy of the Thai government to extend rubber tree plantation. Despite

climatic and edaphic conditions being very different to those of the original growing region (South of Thailand), rubber tree plantation has extended by about 170 000 ha between 2004 and 2006 (Rantala, 2006). The introduction of rubber tree in the Northeast of Thailand may also contribute to important land-use changes affecting soil and water resources. In this area the average annual rainfall (1.1–1.2 m) does not completely meet the minimal requirements for rubber tree (1.3 m), and therefore it is necessary to design a wise water management to be able to ensure sustainable rubber tree farming. In order to achieve this practical goal, numerical modeling of water flow in soils is a valuable tool, to quantify precisely the water balance and the different mechanisms involved (Soares and Almeida, 2001; Antonino et al., 2004; Anuraga et al., 2006) and therefore to try to forecast the evolution of the system, as the new land use may be leading to changes in the general water balance. In order to achieve accurate quantification of these changes with modeling it is therefore necessary to estimate precisely the hydrodynamical properties of the vadose zone.

Several laboratory methods are commonly used to determine the hydraulic properties of soil, like the pressure plate method (Klute and Dirksen, 1986; Bittelli and Flury, 2009) to determine the retention curve, and hydraulic conductivity measurements like hot air, crust, one-step outflow, sorptivity based methods (Stolte et al., 1994). Some in situ methods have mainly been developed to measure hydraulic conductivity in the field like the tension disc infiltrometer (Perroux and White, 1988; Akeny et al., 1991; Angulo-Jaramillo et al., 2000). In any of these cases the determination of the hydraulic parameters of unsaturated soil is always tedious and time consuming. Therefore the quest for alternative methods of determination is a research issue. For example the development of pedotransfer functions (PTFs) which provide relationships between soil hydraulic parameters and more easily measurable properties such as particles size distribution, has become successful amongst soil scientists and hydrologists (Bouma, 1989; Pachepsky et al., 2006). They are mainly based on the textural properties of soil but show some inadequacy in describing structural aspects of soil. Consequently, specific methods taking into account structural properties have been developed to tackle

this problem. For example, the Beerkan method (Haverkamp et al., 1996; Braud et al., 2005) is a field and laboratory measurement method aimed to determine retention curve and hydraulic conductivity curve by particle size distribution and single ring infiltration data, in order to describe the contribution of the texture and the structure to hydraulic properties. But, the main interest of this method is to provide an efficient and low cost estimation of soil hydraulic properties. These basic data are processed with the BEST algorithm according to this theory (Lassabatere et al., 2006), to provide acceptable estimations of hydraulic parameters to a complete characterization of hydraulic characteristic curves. Finally we compared it to a laboratory evaporation method inspired by the method proposed by Wind (1968), which is based on an evaporation measurement to estimate soil water retention and hydraulic conductivity. Wind's method has become very popular and constantly improved by the introduction of inverse modeling (Tamari et al., 1993; Simunek et al., 1998; Richard et al., 2001) and has been adapted for infiltration procedures (Bruckler et al., 2002). Though hydraulic conductivity being well predicted for the dry part of the curve, Wind's method is generally inadequate near saturation for hydraulic gradients being to low (Tamari et al., 1993; Wendroth et al., 1993; Richard et al., 2001). In this study we considered only part of the evaporation technique, in order to determine experimentally the retention curve.

Land uses changes are known to modify soil properties and especially the unsaturated soil hydraulic characteristics (Zimmermann et al., 2006; Price et al., 2010) as the soil structure might be affected. Different land managements such as rubber tree plantation, pasture or natural forest on the same soil series are expected to show very different soil properties. The purpose of this study is to verify this hypothetis and to compare the performance of different measurement techniques for estimating the soil-hydraulic properties of top soil in a typical mini watershed of North East Thailand, in order to accurately model soil water flow.

## 2 Materials and methods

### 2.1 Site and soil description

The study area is set-up in a small watershed located near Ban Noon Tun, Phra Yuen District, Khon Kaen Province, Thailand (16°19′43.90″ N, 102°45′07.91″ E) at about 19 km southwest of the city of Khon Kaen. This area is submitted to a tropical savanna climate, with an annual rainfall of 1.3 m and 1.96 m in 2007 and 2008 respectively, and an average annual temperature of 29 °C. The site is located in the typically undulating landscape of Northeast Thailand, with an elevation ranging from 165 to 181 m above medium sea level and average slope of 3.5 % (Fig. 1). The surface area of the mini watershed is estimated to 200 m × 104 m, where most of the surface is covered with rubber trees (*Heavea Brasiliensis*) and ruzi grass (*Brachiaria Ruziziensis*) cultivated for seeds. The area dedicated to rubber tree plantation is approximately 120 m × 104 m and previously the land was planted with jute (*Corchorus capsularis*), cassava (*Manihot esculenta*) and ruzi grass. Following the governmental policy and the bright economical perspectives for the farmers, the soil use has changed to rubber tree plantation in 2004.

The soil is generally shallow; in the upper part of the toposequence the soil thickness is about 1.70 m, 0.90 m mid-slope, and 2.5 m downslope. The soil texture is classified as sand to sandy clay loam, with bulk density ranging from 1.38 to 1.54 × 10$^3$ kg m$^{-3}$. According to the USDA classification system the soil fitted into 3 subgroups i.e. Typic Haplustult, Arenic Paleustalf, and Typic Paleustult. The soil profile is constituted of an unstructured superficial sandy layer with low clay and organic matter contents, overlying a 0.20 to 0.50 m thick grey clayey layer colored locally with red weathered material from the bedrock (Wiriyakitnateekul et al., 2009) The bedrock which is also probably the parental material, is a fine red sandstone or siltstone, containing clay minerals and feldspars (orthoclase), thoroughly weathered in its upper part, and densely fractured. The physical and chemical properties of the soil measured in the laboratory (Table 1), show that the texture of the top soil is sandy for rubber tree (upslope and mid-slope)

Full Screen / Esc

Printer-friendly Version

Interactive Discussion

and ruzi grass and loamy sand for rubber tree (downslope) and forest. Moreover they show slightly acidic soils with very low organic matter content, though slightly higher in the forest (Table 1).

The first situation considered for measuring soil hydraulic properties was a toposequence of 300 m along a gentle slope (3 %) in the rubber tree plantation (i.e. RT site, Fig. 1) where three positions were selected; up-slope, mid-slope, and down-slope. Next to the rubber tree plantations, important extensions of ruzi grass pasture are still present in this small watershed, which are ploughed once a year, during the rainy season, just before sowing. The second measurement site was located in a ruzi grass pasture plot close to the rubber tree plantation (i.e. RG site, Fig. 1). The third measurement site was located in the upper part of the watershed where an original Dipterocarpus forest has been conserved (i.e. F site, Fig. 1). Experimental soil water flow measurements devices, namely tensiometers with pressure sensors (SKT 850T, SDEC, Reignac sur Indre, France) and soil moisture sensors (Enviroscan probe, Sentek, Stepney SE, Australia) were installed in the different sites (RT up-, mid-, down-slope, RG and F), and monitored every two hours continuously from 2007 to 2009. Tensiometric data were recorded at 0.10, 0.25, 0.40, 0.60 and 1.10 m and soil moisture was measured at 0.10, 0.30, 0.50, 0.70, 0.90, 1.10 and 1.40 m. Meteorological data (rainfall, temperature, air humidity, wind speed, solar radiation) were recorded continuously at a single site in the small watershed (Fig. 1). In each experimental site (RT up-, mid-, down-slope, RG and F), Beerkan infiltration experiments were performed in the field during the dry season, from November 2007 to February 2008 and soil cylinders were collected for laboratory evaporation method measurements. The soil volumetric water content at 0–0.10 m deep was 0.01 ($m^3 m^{-3}$) for RT up-slope and F and 0.02 for the other sites.

## 2.2 Estimation of soil unsaturated hydraulic properties

Modeling and quantifying water flow in vadose zone is mostly described by Richards' equation (Richards, 1931), and in order to solve this equation it is required to determine (i) the soil water retention function, relating the pressure head to the soil water content

$h(\theta)$:

$$S_e = \left(\frac{\theta - \theta_r}{\theta_s - \theta_r}\right) = (1 + (\alpha h)^n)^{-m} \tag{1}$$

$$m = 1 - \frac{k}{n} \tag{2}$$

and (ii) the hydraulic conductivity based on Brooks and Corey (1964) model (Eq. 3)

$$\frac{K(\theta)}{K_s} = (S_e(\theta))^\eta \tag{3}$$

or van Genuchten relationship:

$$K(\theta) = K_s S_e{}^l \left[1 - \left(1 - S_e{}^{1/m}\right)^m\right]^2 \tag{4}$$

These equations are defined by several parameters where $h$ is the pressure head [L], $S_e$ the effective saturation [–], $\theta$ [$L^3 L^{-3}$] is volumetric water content, $\theta_r$ and $\theta_s$ are residual and saturated water content, $m$ [–], and $n$ [–] are shape parameters and, $k$ is an integer usually chosen to be 1 (Mualem, 1976) or 2 (Burdine, 1953); $\alpha$ [$L^{-1}$] is the scale fitting parameter; $K_s$ [$L T^{-1}$] is the saturated hydraulic conductivity, $l$ [–] and $\eta$ [–] other shape parameters, with $l$ usually considered to be 1/2.

### 2.2.1 The Beerkan method

The experimental procedure of this method consisted of two distinct processes i.e. the soil particle size distribution analysis and a single ring infiltration test. According to the theory developed in Braud et al. (2005) and Lassabatere et al. (2006) 3-D axi-symetric infiltration was realized with a zero pressure head at the soil surface. It was achieved with pulse flux of small volumes of water and the infiltration tests were performed in situ with a 0.102 m diameter cylinder. The infiltration cylinder was driven firmly into the soil

for about 0.01 to 0.02 m in order to prevent lateral loss of water from infiltration cylinder. A series of constant volume of water ($120 \times 10^{-6}$ m$^3$) was poured into the cylinder and time was recorded after each volume of water was completely infiltrated. Each volume represented a maximum of 0.015 m of pounding pressure at soil surface when the cylinder was freshly refilled. Haverkamp et al. (1998) showed that small variations in pounding pressure did not influence significantly the infiltration rate and the surface pressure head in the present case could be considered to be nil. The soil surface microtopographic irregularities in a cylinder of 0.102 m diameter are therefore negligible for accounting to the surface pressure. The time reading for each added volume was recorded precisely when the last free water puddle vanished completely from the soil surface. A new volume was added immediately to ensure continuous water supply. This procedure was continued until the steady-state infiltration rate was reached. Undisturbed and disturbed soil sample were collected at the test spot to determine dry bulk density, particle size distribution by sedimentation method, initial ($\theta_0$) and final ($\theta_s$) volumetric water content. Six replicate infiltration tests have been conducted in each site. The results were analyzed with BEST algorithm (Lassabatere et al., 2006) in order to obtain both, the water retention curve (Eq. 1) with Burdine condition, $k = 2$ (Eq. 2) and the hydraulic conductivity (Eq. 3). The details of this calculation procedure are presented in Appendix A. However in order to compare the results with other methods and to be able to use these parameters in numerical models like Hydrus1D (Simuneket et al., 2005), the curves obtained with BEST were then adjusted to van Genuchten with Mualem conditions ($k = 1$ in Eq. 2) following Mubarak et al. (2009).

## 2.2.2 Disc infiltrometer

This common field technique to measure saturated hydraulic conductivity was used in the different sites with the device SW080 B (SDEC, Reignac-sur-Indre, France), with a 20 cm diameter infiltration disc. In order to calculate saturated hydraulic conductivity with the multipotential method (Perroux and White, 1988; Smettem and Clothier, 1989), the infiltration measurements have been realised for two different suctions

values and interpreted with Wooding's method (Wooding, 1968; Akeny et al., 1991; Angulo-Jaramillo et al., 2000).

### 2.2.3 Evaporation method

Two undisturbed soil samples were collected in the field at each location (RT up-, mid-, down-slope, RG, F) by driving a PVC cylinder (height 9 cm and diameter 15 cm) into the previously wetted soil surface. The soil cylinders were air-dried ensuring the soil structure was preserved, and slowly saturated with tap water to control the initial water content. Four micro-tensiometers ($3 \times 10^{-2}$ m length $\times 1.5 \times 10^{-2}$ m in diameter) filled with de-aired water were connected to pressure transducers (model Honeywell 15 PSI, Honeywell Aerospace Plymouth, Plymouth MN) and inserted into the soil sample at four depths: at 0.011, 0.034, 0.056 and 0.079 m from the top of the soil sample. The cylindrical soil sample was dried from the upper surface at an air temperature of 30 °C in very slow evaporation conditions with a constant evaporation rate of $8 \times 10^{-9}$ m s$^{-1}$. Pressure and the weight were recorded during evaporation at a regular time interval (30 min) on a data logger (Model CR10, Campbell Scientific, Logan UT). The measurements continued until reaching the air entry limit of the ceramic cup of the tensiometer. The soil was removed from PVC cylinder and oven-dried at 105 °C during 24 h and final water content and dry bulk density were calculated. As evaporation rate was set to be slow with a quasi steady-state flux, pressure head gradient in the soil sample was close to zero, with uniform pressure head profile. Therefore it was legitimate to derive the retention curve from the average tension measured in the 4 tensiometers and from the water content variation during the drying of the soil cylinder. The relationship of van Genuchten (1980), (Eq. 1) with Mualem condition ($k = 1$) has been used to fit to the experimental water retention curves.

### 2.2.4   The inverse method

The original method of Wind is known for introducing some biases in the calculation of the hydraulic conductivity near saturation especially as the hydraulic gradient is low (Tamari et al., 1993; Wendroth et al., 1993; Richard et al., 2001). Therefore, the same experimental data set as for the evaporation method was used to derive the soil hydraulic parameters by numerical inverse modeling with Hydrus1D (Simuneket et al., 2005). The height of the simulated domain was set to 0.09 m, with 4 observation points corresponding to the positions of the tensiometers in the soil cylinder. The boundary conditions were set to Neumann conditions, namely the lower boundary condition was set to zero-flux and the upper boundary condition was set to the experimental evaporation flux. The inversion procedure is based on the minimization of an objective function describing the difference between observed and computed values. The estimated unsaturated soil characteristics were chosen to be described by van Genuchten (1980) relationship (Eqs. 1 and 4) with Mualem condition ($k = 1$, Eq. 2). In order to improve the fitting procedure, the values of $\theta_r$, $\theta_s$, $n$, and $\alpha$ obtained with the evaporation method and the values of $K_s$ obtained with disc infiltrometer were used as initial guesses for the inversion procedure. The water content parameters $\theta_r$ and $\theta_s$ were kept fixed whereas the parameters n, $\alpha$, $K_s$ were fitted and $l$ was set to 0.5.

### 2.2.5   Pedo-transfer function

Many pedo-transfer functions relating simple particle size distribution (PSD) to the soil water characteristics (SWC) and especially the water retention curve have been developed in the last decades (Pachepsky and Rawls, 2003). The model proposed by Arya et al. (1999) based on the original work of Arya and Paris (1981) is a partly physically based model, deriving from the pore size distribution of a soil from the PSD data,

according to the following equation:

$$r_i = R_i \sqrt{\frac{2en_j^{1-\alpha_i}}{3}} \tag{5}$$

where $r_i$ is the mean pore radius and $R_i$ the mean particle radius for the $i$th particle size fraction, $e$ is the void ratio of the natural structured soil sample, $n_i$ is the equivalent number of spherical particles in the $i$th particle size fraction, and $\alpha_i$ a scale factor. The calculation details for these parameters are presented in the Appendix B. Finally the pore radii, $r_i$, are converted into equivalent pressure heads, $h_i$ using the capillary rise equation:

$$h_i = \frac{2\eta \cos\Theta}{\rho_{\mathrm{w}}gr_i} \tag{6}$$

where $\eta$ is the water surface tension at the air water interface, $\Theta$ is the contact angle, $\rho_{\mathrm{w}}$ is the density of water, and $g$ is the acceleration due to gravity. The volumetric water content, $\theta_i$ ($\mathrm{m^3\,m^{-3}}$), is obtained from successive summation of water-filled pore volumes according to

$$\theta_i = (\varepsilon S_{\mathrm{w}}) \sum_{j=1}^{j=i} w_j \tag{7}$$

where $\varepsilon$ is the total porosity ($\mathrm{m^3\,m^{-3}}$), and $S_{\mathrm{w}}$ is the saturation rate.

## 2.3   Evaluation of the methods

Experimental soil water flow measurement devices, namely tensiometers and soil moisture sensors (Enviroscan probe, Sentek, Stepney SE, Australia) were installed

**Estimating unsaturated hydraulic properties**

S. Siltecho et al.

in the different soil situations, and were continuously recorded every two hours for several years. In order to evaluate the goodness of the soil parameters estimation methods, a reference was needed. The final use for these parameters was modeling of soil water flow and no intrinsic correct values were known, so these parameters were evaluated by modeling with Hydrus1D, a robust and well documented software (Simunek et al., 2005), and comparing modeled results with experimental data. The calculation has been performed on a uniform 0.35 m deep domain with two tensiometric boundary conditions measured in the field at 0.10 m as upper boundary condition and at 0.45 m for the bottom boundary condition. This choice has been motivated by the necessity to perform the simulation with well constrained boundaries. The development of matric potential during an almost one-year period was calculated for the intermediate tensiometer located at 0.25 m. These calculations were performed with the combination of the unsaturated soil parameters measured with the different methods (i.e. Beerkan, disc infiltrometer, PTF, evaporation and inverse methods) and were compared to the experimental tension values measured in the 5 different locations (i.e. in the forest, ruzi grass, and the three positions in the rubber plantation). Four criteria generally proposed were used to evaluate the performance of modeling (Table 2), namely the root mean squared error (RMSE), the coefficient of determination (CD), the modeling efficiency index (EF) and the coefficient of residual mass (CRM) (Loague and Green, 1991; Kim et al., 1999).

## 2.4 Statistics

Estimated variables, namely saturated hydraulic conductivity ($K_s$), parameter $\alpha$ and parameter $n$ were analyzed using standard statistics to calculate their mean and coefficient of variation values. Statistical R package (2008) was used to test normality of data frequency distribution with Anova test, but as the number of samples was limited (from 3 to 10 samples per method tested in each site) Kruskal–Wallis non parametric tests were also used to check the hypothesis of same continuous distribution for the

different cases. This test allows to test equality between means or medians of different groups of data, without presuming any specific hypothesis on the distribution.

## 3 Results and discussion

### 3.1 Beerkan method

With a simple 3-D infiltration experiment combined with particle size distribution analysis, BEST software (Lassabatere et al., 2006) derived the main shape parameter $n$ and scale parameter $K_s$ and $\alpha$ describing the unsaturated hydraulic properties. The results displayed in Table 3 show relatively low variation between the different sites. Saturated hydraulic conductivity ($K_s$) ranged from 5.59 to $10.23 \times 10^{-6} \, \mathrm{m \, s^{-1}}$ within the different sites and showed a clear gradient along the slope in the rubber tree plantation. The highest value of $K_s$ were found upslope and the lowest downslope, probably due to the accumulation of finer particles in the lower part, as mentioned by other authors (Heddadj and Gascuel-Odoux, 1999; Jing et al., 2008) describing topographic variation of hydraulic conductivity. Average $K_s$ values were found to be very similar for the soil in ruzi grass and in forest (5.84 and $5.93 \times 10^{-6} \, \mathrm{m \, s^{-1}}$, respectively) though the standard deviation was much higher for ruzi grass than for forest ($3 \times 10^{-6}$ and $9 \times 10^{-7} \, \mathrm{m \, s^{-1}}$, respectively). Along the slope, the relative standard error on $K_s$ was also quite high with values ranging between 49 and 62 %. The retention curve parameters, $\alpha$ and $n$ also showed little variation between the different sites; for most of the cases the average value of $\alpha$ was 1.4 or $1.5 \times 10^{-4} \, \mathrm{m^{-1}}$, except for the forest (F) where $\alpha$ displayed higher values ($2.8 \times 10^{-4} \, \mathrm{m^{-1}}$). The shape parameter $n$ followed a similar trend as $K_s$, namely decreasing values along the slope (2.33, 2.26 and 2.06 respectively in up-, mid- and downslope positions). Outside the plantation, average value for $n$ in ruzi grass (R) was within the range previously observed, namely 2.23, but it was significantly lower in the Forest situation with a value of 2. Normalized or scaled retention curves (Fig. 3d) were established with dimensionless values of water content ($S_e$) and of the matric potential

Full Screen / Esc

Printer-friendly Version

Interactive Discussion

$(h^* = h\alpha)$, in order to simplify the retention curve $h(\theta)$, and to compare the shape parameters. They showed very similar shapes for all the locations with a small shift for the F soil samples, indicating differences in shape parameters for the soil in Forest resulting from a slight higher clay content.

## 3.2 Disc infiltrometer

Results obtained for $K_s$ with disk infiltrometer showed a behavior similar to that with the Beerkan method, namely a progressive decrease down the slope in the rubber tree plantation. Though the actual values for $K_s$ were systematically lower, namely 6.9, 5.1 and $3.5 \times 10^{-6}\,\mathrm{m\,s^{-1}}$ from upslope to downslope positions respectively (Table 2). The average values of $K_s$ in the Forest and Ruzi grass were larger than those for the Beerkan method (6.65 and $6.93 \times 10^{-6}\,\mathrm{m\,s^{-1}}$ respectively). The relative standard errors for this method were significantly larger than for the Beerkan method, with values ranging from 66 to 90 %.

## 3.3 Evaporation method and associated inverse method

Theoretically the water retention curve obtained from the evaporation method could be considered as a reference for it corresponds to direct experimental data with no model assumed a priori. In order to compare the results more easily with the other methods, the van Genuchten model with Mualem conditions was used to fit to the experimental retention curves. Parameter $\alpha$ varied only in a very narrow interval between $1.8 \times 10^{-4}$ and $2.5 \times 10^{-4}\,\mathrm{m^{-1}}$ and was found to be equal for both methods. Nevertheless the values were found to be slightly larger than for the Beerkan method. Values for shape parameter $n$ are significantly different between the two methods with higher values for evaporation method. By comparison the $n$ values obtained with the Beerkan method are much lower than those derived from evaporation and inverse methods. The scaled infiltration curves depicted in Fig. 3c for the evaporation method show clearly slight differences between the different situations. A single soil sample from the RT in mid-

slope position was sticking out with a noticeably larger value for $n$. Saturated hydraulic conductivity obtained with the inverse method was much more important than when determined with other methods as it ranged from 10 to $22 \times 10^{-6}\,\mathrm{m\,s^{-1}}$. Regarding $K_\mathrm{s}$ along the slope the same pattern was found, namely showing an increase along the slope from the bottom to the upper position. Unlike the disc infiltrometer and Beerkan methods, $K_\mathrm{s}$ for ruzi grass and for forest soils were found to be very different, with a very high $K_\mathrm{s}$ value for Ruzi grass; $22 \times 10^{-6}\,\mathrm{m\,s^{-1}}$ instead of $6 \times 10^{-6}\,\mathrm{m\,s^{-1}}$ with the other methods.

## 3.4 Arya and Paris method

Van Genuchten water retention parameters were fitted on the experimental curves and showed little variation for parameter $\alpha$ between the different sites, reflecting a low variability of PSD. On the other hand, the values for $\alpha$ were found to be significantly lower than for the other estimation methods. The shape parameter n showed very high variability with average values ranging from 1.82 for RG to 3.35 for RTmid and important standard deviation running from 3 to 67 %. The scaled retention curves (Fig. 3b) for this method were very similar, though the Forest soil samples showed a slightly particular behavior. Nevertheless, when all are represented on the same graph, the slight variations of scaled retention curves corresponding to the location of the soil samples, seemed negligible compared to the differences due to the measurement methods (Fig. 3a). The value of shape parameter $n$ represented by the slope of the retention curve was lowest for the Beerkan method, intermediate for Arya method and highest for the evaporation method.

## 3.5 Statistical analysis

The statistical analysis of the van Genuchten unsaturated soil water parameters for the different locations with the different experimental techniques was performed with the Kurskal–Wallis non parametric method. Both $\kappa^2$ and $p$ values (Table 4) showed

Discussion Paper | Discussion Paper | Discussion Paper | Discussion Paper

clearly that measured unsaturated soil water parameters were highly dependent on the measurement techniques. As already pointed out on the scaled retention curves, parameter $n$ seemed to be the most dependent on the type of method, considering the high value of $\kappa^2$ and extremely low $p$ value. The shape parameter $\alpha$ showed the highest $\kappa^2$ value, but saturated hydraulic conductivity $K_s$ is also highly dependent on the measurement method. The influence of location was found to be secondary or even negligible, with $p$ value of 0.11, 0.94 and almost 1 for $\alpha$, $n$ and $K_s$, respectively, except for $\alpha$ showing a relatively high value for $\kappa^2$ (7.15) but still under the acceptable limit (9.49) for the corresponding degrees of freedom (4). Saturated hydraulic conductivity $K_s$ was therefore not a discriminating parameter for the different situations, whereas parameter $n$ tended to show an evolution with the different sites. When data were considered globally regrouping all the measurement methods the variability of the results was higher considering the measurement method rather than the measurement location. When studied separately for each measurement method (Table 4), some parameters seemed to discriminate clearly the different sites. For example, with Beerkan method, the shape parameter $n$ appeared to be significantly different for the different sites. With the pedotransfer function of Arya and Paris, scale parameter $\alpha$ was the most discriminating parameter with an extremely low $p$ value, though parameter $n$ also showed a low $p$ value ($< 0.05$). In both cases it was shown that the particle size distribution and the derived parameters were significantly different at the various sites for these two measurement methods. With the others, no clear discrimination between the different sites was observed as the $p$ values very high, between 0.15 and 0.86.

## 3.6 Modeling validation

Unsaturated soil water parameters are generally determined to use in mathematical models simulating soil water flow. Their evaluation was therefore performed with Hydrus1D, and the computed matric potentials at 0.25 m were compared to the experimental data. The different locations could be divided in two distinctive groups where (i) infiltration was strictly 1-D with vertical water flow, corresponding to the Forest and Ruzi

Title Page

Abstract | Introduction

Conclusions | References

Tables | Figures

|◄ | ►|

◄ | ►

Back | Close

Full Screen / Esc

Grass and (ii) with a possible lateral flow component due to the slope in Rubber Tree plantation. The results obtained in the Forest and the Ruzi Grass sites showed good conformity with the experimental data (Fig. 4) with RMSE values less than 40 hPa, and EF values close to unity especially for the Forest site (0.83–0.95). The numerical simulations obtained with unsaturated soil water parameters issued from the different methods, show very little differences. In both cases (F and RG) the best fit was obtained with parameters derived from the combination of the Arya and Paris method for the retention curves and Disc infiltrometer for the hydraulic conductivity. Simulations performed with parameters from the Beerkan method showed a slightly higher RMSE value, whereas the results obtained with the evaporation method based parameters seemed to fit worse to experimental data. These trends were confirmed by the other modeling evaluation indexes (DR, EF). CRM showed a systematic small negative value for the Forest site, regardless of the measurement method, indicating an underestimation in the computed matric potential values. The scatter plots of computed vs. experimental matric pressure heads (Fig. 5) showed a good agreement for all models in the forest and a slight underestimation for the high values in the ruzi grass. For the rubber tree plantation, concordance between computed results and experimental data, was much worse (Figs. 4 and 5). The general trend was preserved but often overestimated compared to experimental data as depicted in Fig. 4 and quantified by CRM in Table 5. During the rainy season the fit between computed and experimental matric potential was generally better than during the drier period (Fig. 5). This discrepancy can be explained mainly by the slope in the rubber tree plantation and the inevitable subsurface lateral flow. Therefore the water flow in the field was not 1-D and could not be computed adequately; in up- and mid slope position water was lost laterally and accumulated in the downslope position. Nevertheless when lateral flow was taken into account in a 2-D simulation with Hydrus2D (Seltacho et al., 2013) computed and experimental values fitted well. In any case, when contemplated from a yearly time scale, the differences between the different methods for simulating the water flow in soil seemed negligible in terms of water stock. Regardless whether the computed

results fitted the experimental data like for Forest and Ruzi Grass, or did not as with the Rubber Tree plantation, no method could clearly stand out as being more efficient than any other one in modeling water flow for these different situations. These results are informative on the non-uniqueness of the parameters for modeling water flow in soil. Despite not describing exactly the development of soil water potential, different combinations of soil parameters lead to very similar results when used in Hydrus1D at a yearly time scale. The efforts to determine the soil hydraulic parameters precisely can therefore be seriously questioned. In any case to improve the modeling performance for longer time series or to forecast different scenarios, the parameters need to be adjusted by inverse modeling (Seltacho et al., 2013). Moreover these results also showed that for the considered time scale, hysteresis phenomena were negligible. In fact the parameters determined with some methods should be representative of the drainage scanning curve for $h(\theta)$ and/or $K(\theta)$ curves (Evaporation method, inverse method, Arya and Paris method) and others should represent the imbibition scanning curve (Beerkan, Disc infiltrometer). Generally hysteresis affects parameter $\alpha$ of retention curve with a commonly accepted relationship described by several authors (Kool et al., 1987; Nielsen and Luckner, 1992; Maqsoud et al., 2012): $\alpha_w \simeq 2\alpha_d$, where indices w and d account for wetting and drying respectively. Results in Table 4 did not show this type of relationship, despite sandy soils being known to be prone to exhibit strong hysteretical properties.

## 4  Conclusions

In order to determine the unsaturated hydraulic properties of soil for different land use, several experimental methods have been used in a small watershed in Northeast Thailand. They included in laboratory methods like evaporation method, inverse methods and PTF (Arya et al., 1999) and also field evaluations like Beerkan method and disc infiltrometer. A decrease in hydraulic conductivity down the slope in the rubber tree plantation was systematically observed, and could probably be related to translocation

of finer particles downslope (Wiriyakitnateekul et al., 2009). Despite showing slightly higher levels of organic matter and unlike what would commonly be expected, forest soil had the lowest hydraulic conductivity. The higher content in finer particles (clay and silt) was most probably responsible for lower $K_s$ values in the Forest site and in some extent in the Ruzi grass site. During the early stages of the rubber tree plantation the soil surface was not covered and therefore more vulnerable to erosion. The fine soil particles were translocated downslope and down the soil profile. Statistical analysis of the results obtained during this study showed clearly that significative differences in VG parameters measurements appeared depending on the measurement method. Though the impact of land use and position was not completely negligible, the primary factor for measurement variability was found to be in the experimental methods. It was stated that the actual values of VG parameters depend on the method employed to determine them. However, when each measurement method was considered separately the discrimination by site was significant for Beerkan method and Arya's PTF method. For both methods being based on particle size distribution, parameters $n$ and $\alpha$ respectively could discriminate the different sites. Unsaturated soil properties of this sandy soil seemed to be governed mainly by textural parameters related to the pedogenesis rather than by structural properties associated to land-use and management. The final use of these VG parameters was to use them in Hydrus to compute the water balance at these different sites. This study showed clearly that the uniqueness of VG parameters did not apply in this case as many different combinations provided similar or equivalent results when a yearly time scale was considered. The simulation results obtained with the parameters derived from different methods were generally equivalent when the different validation parameters were considered. In any case to perform efficient and reliable modeling of water flow in soil, these parameters should be carefully adjusted by inverse modeling procedures on experimental data over a time series describing contrasted situations and then validated. The measured VG parameters should be used as appropriate first guess values for the inverse modeling procedure. No single method could definitively be contemplated as producing better results than the others.

It should therefore be recommended to use the easiest and cheapest methods for the experimental evaluation of the first set of VG parameters and in this case Beerkan method would surely be the best option. The important land use changes taking place in Northeast Thailand can therefore be evaluated easily with numerical modeling and the consequences of rubber tree plantation on the water balance at different scales can therefore be predicted (Seltacho et al., 2013).

**Appendix A: Determination of *m*, *n* and *η* from textural data**

Particle size distributions with at least 5 fractions (clay, fine silt, coarse silt, fine sand, coarse sand) were determined by sieving the soil. The data of particle size provide the cumulative frequency distribution ($F(d)$) as a function of particle diameter d to be fitted with the model proposed by Haverkamp et al. (1998)

$$F(d) = \left[ 1 + \left( \frac{d_g}{d} \right)^N \right]^{-M} \tag{A1}$$

with $M = 1 - \frac{2}{N}$ where $d$ is particle diameter [L], $d_g = 1/\alpha$ is a scale parameter for particle diameter [L], $M$ and $N$ are shape parameters, determined by least square optimization technique. The shape parameter for water retention curve $m$ and $n$ estimated following Zataráin et al. (2003) and Lassabatere et al. (2006):

$$P_M = \frac{MN}{1+M} \tag{A2}$$

$$P_m = \frac{mn}{1+m} \tag{A3}$$

where *mn* is a shape parameter of the water retention curve and *MN* is a shape parameter from the particle size curve.

$$P_M = (1 + \kappa) P_m \tag{A4}$$

$$\kappa = \frac{2s - 1}{2s(1 - s)} \tag{A5}$$

where $s$ is the solution of the non-linear equation by Fuentes et al. (1998):

$$(1 - \varepsilon)^s + \varepsilon^{2s} = 1 \tag{A6}$$

where $\varepsilon$ is soil porosity. The shape parameter $\eta$ can estimated from

$$\eta = \frac{2}{mn} + 2 + p \tag{A7}$$

where $p$ is a tortuosity parameter (Mualem, 1976).

## Appendix B: Determination of of scale parameters $S$ and $K_s$

Considering a 3-D infiltration from a cylindrical source of radius $r_d$, with a zero water pressure, the cumulative infiltration can be described by two distinct equations. One for short term infiltration with a transient two term infiltration rate and the second for the long term infiltration $I_{+\infty}$ with a steady state infiltration rate (Haverkamp et al., 1994). The cumulative short term infiltration equation is described as follows:

$$I(t) = S\sqrt{t} + \left( AS^2 + BK_s \right) t \tag{B1}$$

and the corresponding instant infiltration rate $q$:

$$q(t) = \frac{S}{2\sqrt{t}} + \left( AS^2 + BK_s \right) \tag{B2}$$

The steady state infiltration

$$I_{+\infty}(t) = \left(AS^2 + BK_s\right) t + C\frac{S^2}{K_s} \qquad \text{(B3)}$$

Where $A$, $B$, $C$ are

$$A = \frac{\gamma}{r_d(\theta_s - \theta_0)} \qquad \text{(B4)}$$

$$B = \frac{2-\beta}{3}\left[1 - \left(\frac{\theta_0}{\theta_s}\right)^\eta\right] + \left(\frac{\theta_0}{\theta_s}\right)^\eta \qquad \text{(B5)}$$

$$C = \left\{2\left[1 - \left(\frac{\theta_0}{\theta_s}\right)^\eta\right](1-\beta)\right\}^{-1} \ln\left(\frac{1}{\beta}\right) \qquad \text{(B6)}$$

Where $\beta$ and $\gamma$ are equal 0.6 and 0.75 respectively when $\theta_0 < 0.25\theta_s$. The BEST algorithm (Lassabatere et al., 2006) estimates $S$ and $K_s$ through an iterative optimizing process, for which both transient and steady state flow equations can be considered valid (Eqs. B1–B6). Parameter $\alpha$ is then estimated by:

$$\alpha = -\frac{C_p(\theta_s - \theta_0)(K_s - K_0)}{S^2} \qquad \text{(B7)}$$

$$C_p = \Gamma\left(1 + \frac{1}{n}\right)\left\{\frac{\Gamma\left(m\eta - \frac{1}{n}\right)}{\Gamma m\eta} + \left(\frac{\Gamma\left(m\eta + m - \frac{1}{n}\right)}{\Gamma(m\eta + m)}\right)\right\} \qquad \text{(B8)}$$

Where $\Gamma$ is the usual Gamma function.

## Appendix C: Determination of parameters for the Arya et al. model

The void ratio is given by:

$$e = \frac{\rho_s - \rho_b}{\rho_b} \qquad \text{(C1)}$$

where $\rho_s$ is the particle density and $\rho_b$ is the dry bulk density of the natural structured soil sample. The equivalent number of spherical particles ($n_i$) in the $i$th particle size fraction can be calculated from

$$n_i = \frac{3w_i}{4\pi\rho_s R_i^{\,3}} \tag{C2}$$

where $w_i$ is the fraction solid mass. The scaling parameter ($\alpha_i$) was defined by Arya et al. (1999) as

$$\alpha_i = \frac{\log N_i}{\log n_i} \tag{C3}$$

where $N_i$ is the scale number of hypothetical spherical particles of radius $R_i$ required to trace the tortuous pore length contribute by $n_i$ natural particle in the actual sample. The scale number $N_i$ can be obtained from the particle size distribution using the empirical relationship (Arya et al., 1999)

$$\log N_i = a + b \log \frac{w_i}{R_i^3} \tag{C4}$$

where $a$ and $b$ are empirical parameters according to Arya et al. (1999)

**Estimating unsaturated hydraulic properties**

S. Siltecho et al.

# References

Angulo Jaramillo, R., Vandervaere, J.-P., Roulier, S., Thony, J.-L., Gaudet, J.-P., and Vauclin, M.: Field measurement of soil surface hydraulic properties by disc and ring infiltrometers: a review and recent developments, Soil Till. Res., 55, 1–29, 2000. 6102, 6108

5 Ankeny, M. D., Ahmed, M., Kaspar, T. C., and Horton, R.: Simple field method for determining unsaturated hydraulic conductivity, Soil Sci. Soc. Am. J., 55, 467–470, 1991. 6102, 6108

Antonino, A. C. D., Angulo-Jaramillo, R., Hammecker, C., Netto, A. M., Montenegro, S. M. L. G., Lira, C. A. B. O., and Cabral, J. J. S. P. A.: A simplified water transfer model of the reservoir-ebb tide system, including preferential flow, in the semi-arid region in Northeastern Brazil, J. Hydrol., 287, 147–160, 2004. 6102

10 Anuraga, T., Ruiz, L., Kumar, M. M., Sekhar, M., and Leijnse, A.: Estimating groundwater recharge using land use and soil data: a case study in South India, Agr. Water Manage., 84, 65–76, 2006. 6102

Arya, L. M. and Paris, J. F.: A physicoempirical model to predict the soil moisture characteristics from particle-size distribution and bulk density data, Soil Sci. Soc. Am. J., 45, 1023–1030, 1981. 6109

Arya, L. M., Leij, F. J., Shouse, P. J., and van Genuchten, M. T.: Relationship between the hydraulic conductivity function and the particle-size distribution, Soil Sci. Soc. Am. J., 63, 1063–1070, 1999. 6109, 6117, 6122

20 Bittelli, M. and Flury, M.: Errors in water retention curves determined with pressure plates, Soil Sci. Soc. Am. J., 73, 1453–1460, 2009. 6102

Bouma, J.: Using soil survey data for quantitative land evaluation, Adv. Soil S., 9, 177–213, 1989. 6102

Braud, I., De Condappa, D., Soria, J. M., Haverkamp, R., Angulo-Jaramillo, R., Galle, S., and Vauclin, M.: Use of scaled forms of the infiltration equation for the estimation of unsaturated soil hydraulic properties (the Beerkan method), Eur. J. Soil Sci., 56, 361–374, 2005. 6103, 6106

Brooks, R. H. and Corey, C. T.: Hydraulic properties of porous media, Hydrol. Paper 3, Colorado State University, Fort Collins, 1964. 6106

30 Bruckler, L., Bertuzzi, P., Angulo-Jaramillo, R., and Ruy, S.: Testing an infiltration method for estimating soil hydraulic properties in the laboratory, Soil Sci. Soc. Am. J., 66, 384–395, 2002. 6103

Burdine, N. T.: Relative permeability calculation from pore size distribution data, Petr. Trans. Am Inst. Min. Metall. Eng., 198, 71–77, 1953. 6106

Evett, S., Peters, F., Jones, O., and Unger, P.: Soil Hydraulic conductivity and retention curves from tension infiltrometer and laboratory data, in: Proceedings International Workshop on Characterization and Measurement of the Hydraulic Properties of Unsaturated Porous Media, edited by: van Genuchten, M. T., Leij, F. J., and Wu, L., 541–551, University of Riverside. 1999.

Fuentes, C., Vauclin, M., Parlange, J. Y., and Haverkamp, R.: Soil water conductivity of a fractal soil, in: Fractals in Soil Science, edited by: Baveye, P., Parlange, J. Y., and Stewart, B. A., Lewis Publisher, Boca Raton, FL, 333–340, 1998.

Haverkamp, R., Ross, P. J., Smettem, K. R. J., and Parlange, J.-Y.: Three-dimensional analysis of infiltration from the disc infiltrometer: 2. Physically-based infiltration equation, Water Resour. Res., 30, 2931–2935, 1994. 6120

Haverkamp, R., Arrue, J. L., Vandervaere, J.-P., Braud, I., Boulet, G., Laurent, J. P., Taha, A., Ross, P. J., and Angulo-Jaramillo, R.: Hydrological and thermal behaviour of the vadose zone in the area of Barrax and Tomelloso (Spain): experimental study, analysis and modeling Project UE no EV5C-CT 92 00 90, Laboratoire d'étude des Transferts en Hydrologie et Environnement, Grenoble, 1996. 6103

Haverkamp, R., Bouraoui, C., Zammit, R., Angulo-Jaramillo, R., and Delleur, J. W.: Soil properties and moisture movement in the unsaturated zone, in: The Handbook of Groundwater Engineering, edited by: Delleur, J. W., CRC, Boca Raton, FL, 2931–2935, 1998. 6107, 6119

Heddadj, H. and Gascuel-Odoux, C.: Topographic and seasonal variations of unsaturated hydraulic conductivity as measured by tension disc infiltrometers at the field scale, Eur. J. Soil Sci., 50, 275–283, 1999. 6112

Jing, Y.-S., Zhang, B., Thimm, A., and Zepp, H.: Anisotropy of soil hydraulic properties along arable slopes, Pedosphere, 18, 353–362, 2008. 6112

Kim, D. J., Angulo-Jaramillo, R., Vauclin, M., Feyen, J., and Choi, S. I.: Modeling of soil deformation and water flow in a swelling soil, Geoderma, 92, 217–238, 1999. 6111

Klute, A. and Dirksen, C.: Hydraulic conductivity and diffusivity: laboratory methods, in: Methods of Soil Analysis. Part 1. Physical and Mineralogical Methods, edited by: Klute, A., 2nd Edn., ASA and SSSA, Madison, WI, 687–734, 1986. 6102

Title Page

Abstract | Introduction

Conclusions | References

Tables | Figures

|◄ | ►|

◄ | ►

Back | Close

Full Screen / Esc

Printer-friendly Version

Interactive Discussion

Kool, J. B., Parker, J. C., and van Genuchten, M. T.: Determining soil hydraulic properties from one-step outflow experiments by parameter estimation: I. Theory and numerical studies, Soil Sci. Soc. Am. J., 49, 1348–1354, 1985.

Kool, J. B., Parker, J. C., and van Genuchten, M. T.: Parameter estimation for unsaturated flow and transport models – a review, J. Hydrol., 91, 255–293, 1987. 6117

Lassabatere, L., Angulo-Jaramillo, R., Soria Ugalde, J. M., Cuenca, R., Braud, I., and Haverkamp, R.: Beerkan. Estimation of soil transfer parameters through infiltration experiments – BEST, Soil Sci. Soc. Am. J., 70, 521–532, 2006. 6103, 6106, 6107, 6112, 6119, 6121

Loague, K. M. and Green, R. E.: Statistical and graphical methods for solute transport models, J. Contam. Hydrol., 7, 51–73, 1991. 6111

Maqsoud, A., Bussière, B., Aubertin, M., and Mbonimpa, M.: Predicting hysteresis of the water retention curve from basic properties of granular soils, Geotech. Geol. Eng., 30, 1147–1159, 2012. 6117

Minasny, B. and Field, J. D.: Estimating soil hydraulic properties and their uncertainty: the use of stochastic simulation in the inverse modelling of the evaporation method, Geoderma, 126, 277–290, 2005.

Mualem, Y.: A new model for predicting the hydraulic conductivity of unsaturated porous media, Water Resour. Res., 12, 513–522, 1976. 6106, 6120

Mubarak, I., Mailhol, J. C., Angulo-Jaramillo, R., Bouarfa, S., and Ruelle, P.: Effect of temporal variability in soil hydraulic properties on simulated water transfer under high-frequency drip irrigation, Agr. Water Manage., 96, 1547–1559, 2009. 6107

Nielsen, D. R. and Luckner, L. M.: Theoretical aspects to estimate reasonable initial parameters and range limits in identification procedures for soil hydraulic properties, in: Proc. Intl. Workshop on Indirect Methods for Estimating the Hydraulic Properties of Unsaturated Soils, edited by: van Genuchten, M. T., Leij, F. J., and Lund, L. J., University of California, Riverside, 11–13 October 1989, 147–160, 1992. 6117

Pachepsky, Y. A. and Rawls, W. J.: Soil structure and pedotransfer functions, Eur. J. Soil Sci., 54, 443–452, 2003. 6109

Pachepsky, Y. A. and Rawls, W. J.: Development of pedotransfer functions in soil hydrology, in: Development in Soil Science, Vol. 30, Elsevier, Amsterdam, 542 pp. 2004.

Pachepsky, Y., Rawls, W., and Lin, H.: Hydropedology and pedotransfer functions, Geoderma, 131, 308–316, 2006. 6102

Title Page

Abstract | Introduction

Conclusions | References

Tables | Figures

|◀ | ▶|

◀ | ▶

Back | Close

Full Screen / Esc

Printer-friendly Version

Interactive Discussion

Perroux, K. M. and White, I.: Design for disc permeameters and soil dispersion, Soil Sci. Soc. Am. J., 48, 50–55, 1988. 6102, 6107

Price, K., Jackson, C. R., and Parker, A. J.: Variation of surficial soil hydraulic properties across land uses in the southern Blue Ridge Mountains, North Carolina, USA, J. Hydrol., 383, 256–268, 2010. 6103

R Development Core Team: R: A Language and Environment for Statistical Computing, R Foundation for Statistical Computing, Vienna, Austria, ISBN 3-900051-07-0, available at: http://www.R-project.org (last access: 22 November 2013), 2008. 6111

Rantala, L.: Rubber plantation performance in the Northeast and East of Thailand in relation to environmental conditions, Ms. thesis, Dep. of Forest Ecology, University of Helsinky, Finland, 70 pp., 2006. 6102

Richard, G., Sillon, J., and Marloie, O.: Comparison of inverse and direct evaporation methods for estimating soil hydraulic properties under different tillage practices, Soil Sci. Soc. Am. J., 65, 215–224, 2001. 6103, 6109

Richards, L. A.: Capillary conduction of liquids through porous media, J. Appl. Phys., 1, 318, doi:10.1063/1.1745010, 1931. 6105

Seltacho, S., Sriboonlue, V., Suwanang, N., Wiriyakitnateekul, W., and Hammecker, C.: Quantification and modeling of water flow in sandy soils in Northeast Thailand, in: Advances in Unsaturated Soils, edited by: Caicedo, B., Murillo, C., Colmenares, L. H. J. E., and Berdugo, I. R., CRC Press, London, 573–577, 2013. 6116, 6117, 6119

Simunek, J., Wendroth, O., and van Genuchten, M. T.: Parameter estimation analysis of the evaporation method for determining soil hydraulic properties, Soil Sci. Soc. Am. J., 62, 894–905, 1998. 6103

Simunek, J., van Genuchten, M. T., and Sejna, M.: The HYDRUS-1D software package for simulating the movement of water, heat and multiple solutes in a variably saturated media, Version 3.0 HYDRUS, University of California Riverside, Riverside, California, USA, 2005. 6107, 6109, 6111

Smettem, K. R. J. and Clothier, B. E.: Measuring unsaturated sorptivity and hydraulic conductivity using multiple disc permeameters, J. Soil Sci., 40, 563–568, 1989. 6107

Soares, J. V. and Almeida, A. C.: Modeling the water balance and soil water fluxes in a fast growing Eucalyptus plantation in Brazil, J. Hydrol., 253, 130–147, 2001. 6102

Stolte, J., Freijer, J. I., Bouten, W., Dirksen, C., Halbertsma, J. M., van Dam, J. C., van den Berg, J. A., Veerman, G. J., and Wösten, J. H. M.: Comparison of six methods to determine unsaturated soil hydraulic conductivity, Soil Sci. Soc. Am. J., 58, 1596–1603, 1994. 6102

Tamari, S., Bruckler, L., Halbertsma, J., and Chadoeuf, J. A.: Simple method for determining soil hydraulic properties in the laboratory, Soil Sci. Soc. Am. J., 57, 642–651, 1993. 6103, 6109

van Genuchten, M. T.: A closed form equation for predicting the hydraulic conductivity of unsaturated soils, Soil Sci. Soc. Am. J., 44, 892–898, 1980. 6108, 6109

Wendroth, O., Ehlers, W., Hopmans, J. W., Kage, H., Halbertsma, J., and Wosten, J. H. M.: Reevaluation of the evaporation method for determining hydraulic functions of unsaturated soils, Soil Sci. Soc. Am. J., 57, 1436–1443, 1993. 6103, 6109

Wind, G. P.: Capillary conductivity data estimated by a simple method, in: Water in the Unsaturated Zone, Vol. 1., edited by: Rijtema, P. E. and Wassink, H., Proc. Wageningen Symp. June 1966, Int. Assoc. Scientific Hydrol., Gentbrugge, Belgium, 181–191, June 1968. 6103

Wiriyakitnateekul, W. C., Hammecker, C., Anusontpornperm, S., and Boonrod, S.: Clay mineralogy of soils developed on sandstone along a toposequence in Northeast Thailand, XIV International Clay Conference, Castellaneta Marina, Italy, 520–520, 14–20 June, 2009. 6104, 6118

Wooding, R. A.: Steady infiltration from a shallow circular pond, Water Resour. Res., 4, 1259–1273, 1968. 6108

Zataráin, F., Fuentes, C., Haverkamp, R., and Antonino, A. C. D.: Prediccion de la forma de la caracteristica de humedad del suelo a partir de la curva granulometrica, XII Congreso Nacional de Irrigacion, Zacatecas, Mexico, 13–15 April, 212–219, 2003. 6119

Zimmermann, B., Elsenbeer, H., and De Moraes, J. M.: The influence of land-use changes on soil hydraulic properties: implications for runoff generation, Forest Ecol. Manag., 222, 29–38, 2006. 6103

**Table 1.** Physical and chemical properties of the topsoil in the different sites.

| | sand | silt | clay | bulk density | organic matter | pH |
| | | % | | $\mathrm{kg\,m^{-3}}$ | % | |
|---|---|---|---|---|---|---|
| Rubber tree | | | | | | |
| upslope | 89.3 | 7.1 | 3.5 | $1.39 \times 10^3$ | 0.49 | 6.0 |
| midslope | 88.5 | 7.5 | 4.1 | $1.38 \times 10^3$ | 0.71 | 6.4 |
| downslope | 85.5 | 12.2 | 2.3 | $1.46 \times 10^3$ | 0.70 | 6.4 |
| Ruzi grass | 89.0 | 7.5 | 3.5 | $1.47 \times 10^3$ | 0.63 | 6.6 |
| Forest | 84.6 | 11.1 | 4.3 | $1.54 \times 10^3$ | 0.76 | 6.4 |

**Table 2.** Evaluation criteria for performance of modeling.

| | |
|---|---|
| $\text{RMSE} = \sqrt{\frac{\sum(T_i - M_i)}{N}}$ | Indicates the degree of deviation between the experimental determinations and calculated values tends to zero when the calculated and experimental values tend to be equal |
| $\text{CD} = \frac{\sum_{i=1}^{N}(M_i - \overline{M})^2}{\sum_{i=1}^{N}(T_i - \overline{M})^2}$ | Describes the ratio between the dispersion of experimental determinations and the dispersion of the calculated values, tending towards unity when the experimental and calculated values are consistent |
| $\text{EF} = \frac{\sum_{i=1}^{N}(M_i - \overline{M})^2 - \sum_{i=1}^{N}(T_i - \overline{M})^2}{\sum_{i=1}^{N}(M_i - \overline{M})^2}$ | Indicates if the model provides a better estimate of experimental determinations than the mean value of these determinations The expected value for EF tends towards 1 |
| $\text{CRM} = \frac{\sum_{i=1}^{N} M_i - \sum_{i=1}^{N} T_i}{\sum_{i=1}^{N} M_i}$ | Indicates whether the model tends to overestimate (CRM < 0) or underestimate (CRM > 0) compared to experimental values The optimal value for CMR tends towards zero |

**Table 3.** Means and standard errors for the main van Genuchten parameters with Mualem conditions ($n = 1/\{1 - m\}$) determined for the different methods in the different sites. The number of samples is indicated in parenthesis.

| | $K_s \times 10^{-6}$ (m s$^{-1}$) | | |
| | Beerkan | Disc infiltrometer | inverse |
|---|---|---|---|
| Forest | 5.94 ± 0.94 (3) | 6.65 ± 4.41 (6) | 10.00 ± 2.04 (3) |
| Ruzi | 5.82 ± 3.55 (4) | 6.93 ± 5.45 (7) | 18.48 ± 7.12 (3) |
| RT downslope | 5.59 ± 2.56 (7) | 3.48 ± 2.38 (6) | 10.18 ± 0.82 (3) |
| RT midslope | 8.53 ± 4.22 (11) | 5.11 ± 4.60 (7) | 14.66 ± 8.90 (3) |
| RT upslope | 10.23 ± 6.38 (10) | 6.89 ± 5.31 (6) | 22.06 ± 5.27 (2) |

| | $\alpha$ (m$^{-1}$) | | | |
| | Arya | Beerkan | inverse | evaporation |
|---|---|---|---|---|
| Forest | 1.5 ± 0.9 (6) | 2.8 ± 0.47 (3) | 1.8 ± 0.058 (3) | 1.8 ± 0.058 (3) |
| Ruzi | 0.6 (1) | 1.5 ± 0.56 (10) | 1.87 ± 0.21 (3) | 1.87 ± 0.21 (3) |
| RT downslope | 0.6 (6) | 1.4 ± 0.55 (11) | 1.97 ± 0.21 (3) | 1.97 ± 0.21 (3) |
| RT midslope | 0.54 ± 0.05 (5) | 1.5 ± 0.85 (7) | 1.87 ± 0.21 (2) | 1.87 ± 0.3 (3) |
| RT upslope | 0.5 (5) | 1.5 ± 0.9 (4) | 2.55 ± 0.35 (3) | 1.97 ± 0.21 (3) |

| | $n$ | | | |
| | Arya | Beerkan | inverse | evaporation |
|---|---|---|---|---|
| Forest | 2.83 ± 0.17 (6) | 2.00 ± 0.03 (3) | 2.29 ± 0.09 (3) | 3.29 ± 0.50 (3) |
| Ruzi | 1.82 ± 1.22 (3) | 2.23 ± 0.11 (4) | 2.90 ± 0.44 (3) | 3.82 ± 0.69 (3) |
| RT downslope | 2.72 ± 0.07 (6) | 2.06 ± 0.02 (7) | 2.48 ± 0.29 (3) | 3.20 ± 0.54 (3) |
| RT midslope | 3.35 ± 0.14 (5) | 2.26 ± 0.06 (11) | 2.31 ± 0.08 (3) | 2.96 ± 0.14 (3) |
| RT upslope | 3.17 ± 1.01 (6) | 2.33 ± 0.03 (10) | 2.18 ± 0.02 (2) | 3.32 ± 0.67 (3) |

**Table 4.** Medians and parameters of Kurskal–Wallis, chi-squared ($\kappa^2$), degree of freedom df, and $p$ value for the van Genuchten parameters for different methods and different sites, in General and in Detail for each method, $K_s \times 10^{-6}$ (m s$^{-1}$) and $\alpha$ (m$^{-1}$). B: beerkan, I: inverse, A: Arya, E: evaporation, D: disk.*** indicates statiscally significant difference between values

| | General | Arya | Beerkan | Disc inf. | inverse | Evapor. | $\kappa^2$ | df | $p$ value |
|---|---|---|---|---|---|---|---|---|---|
| | $\alpha$ | 0.6 | 1.6 | – | 1.9 | 1.8 | 28.171 | 3 | $3.34 \cdot 10^{-6}$ |
| | $K_s$ | – | 7.15 | 4.76 | 12.16 | – | 19.364 | 2 | $6.24 \cdot 10^{-5}$ |
| | $n$ | 2.979 | 2.251 | – | 2.331 | 3.117 | 47.981 | 3 | $2.15 \cdot 10^{-10}$ |
| | | Forest | RT down | RT mid | RT up | Ruzi | | | |
| | $\alpha$ | 1.9 | 1.4 | 1.6 | 1.5 | 1.7 | 7.15 | 4 | $1.28 \cdot 10^{-1}$ |
| | $K_s$ | 6,42 | 4,497 | 8,39 | 9,53 | 6,97 | 4.40 | 4 | $3.54 \cdot 10^{-1}$ |
| | $n$ | 2.703 | 2.597 | 2.318 | 2.361 | 2.387 | 1.72 | 4 | $7.87 \cdot 10^{-1}$ |
| method | Detail | Forest | RT down | RT mid | RT up | Ruzi | $\kappa^2$ | df | $p$ value |
| B | $K_s$ | 5.99 | 4.93 | 8.81 | 9.53 | 4.93 | 4.251 | 4 | 0.3731 |
| | $\alpha$ | 2.72 | 1.39 | 1.59 | 1.505 | 1.44 | 6.16 | 4 | 0.1878 |
| | $n$ | 2.01 | 2.06 | 2.26 | 2.33 | 2.20 | 24.54 | 4 | $6.23 \times 10^{-5}$*** |
| I | $K_s$ | 92.68 | 90.00 | 169.86 | 190.60 | 140.28 | 6.35 | 4 | 0.1750 |
| | $\alpha$ | 1.80 | 1.90 | 1.80 | 2.55 | 1.80 | 6.05 | 4 | 0.1955 |
| | $n$ | 2.28 | 2.60 | 2.28 | 2.18 | 3.09 | 6.77 | 4 | 0.1490 |
| A | $\alpha$ | 1.5 | 0.6 | 0.5 | 0.5 | 10.9 | 21.22 | 4 | 0.0003*** |
| | $n$ | 2.84 | 2.72 | 3.4 | 3.553 | 2.84 | 12.97 | 4 | 0.0114 |
| E | $\alpha$ | 1.8 | 1.9 | 1.8 | 1.9 | 1.8 | 1.29 | 4 | 0.8627 |
| | $n$ | 3.07 | 3.42 | 2.89 | 3.60 | 4.01 | 3.47 | 4 | 0.483 |
| D | $K_s$ | 44.51 | 25.85 | 24.24 | 58.03 | 59.71 | 2.71 | 4 | 0.6077 |

**Table 5.** Four modeling evaluation criteria for matric potential for the different situations with the different parameters used in Hydrus1D.

| RMSE (hPa) | Beerkan | Arya-Disc | Inverse | Evaporation-Disc |
|---|---|---|---|---|
| Forest | 33.15 | 27.47 | 24.09 | 42.50 |
| Ruzi grass | 23.02 | 22.56 | 24.45 | 26.71 |
| RT upslope | 64.94 | 60.06 | 65.78 | 64.61 |
| RT midslope | 100.59 | 102.25 | 99.62 | 98.25 |
| RT downslope | 52.63 | 49.06 | 53.21 | 51.22 |
| **DR** | **Beerkan** | **Arya-Disc** | **Inverse** | **Evaporation-Disc** |
| Forest | 1.2 | 1.25 | 1.05 | 1.83 |
| Ruzi grass | 0.56 | 1.05 | 1.42 | 1.65 |
| RT upslope | 0.30 | 0.35 | 0.29 | 0.31 |
| RT midslope | 2.43 | 2.25 | 2.61 | 4.87 |
| RT downslope | 1.33 | 0.27 | 0.24 | 0.27 |
| **ME** | **Beerkan** | **Arya-Disc** | **Inverse** | **Evaporation-Disc** |
| Forest | 0.9 | 0.93 | 0.95 | 0.83 |
| Ruzi grass | 0.62 | 0.76 | 0.72 | 0.66 |
| RT upslope | −2.47 | −1.97 | −2.56 | −2.44 |
| RT midslope | 0.32 | 0.30 | 0.33 | 0.35 |
| RT downslope | 0.85 | −2.06 | −2.60 | −2.43 |
| **CRM** | **Beerkan** | **Arya-Disc** | **Inverse** | **Evaporation-Disc** |
| Forest | −0.03 | −0.06 | −0.09 | 0.08 |
| Ruzi grass | −0.51 | 0.15 | 0.24 | 0.27 |
| RT upslope | 0.69 | 0.62 | 0.70 | 0.69 |
| RT midslope | −0.11 | −0.15 | −0.09 | 0.02 |
| RT downslope | 0.33 | 0.23 | 0.35 | 0.41 |
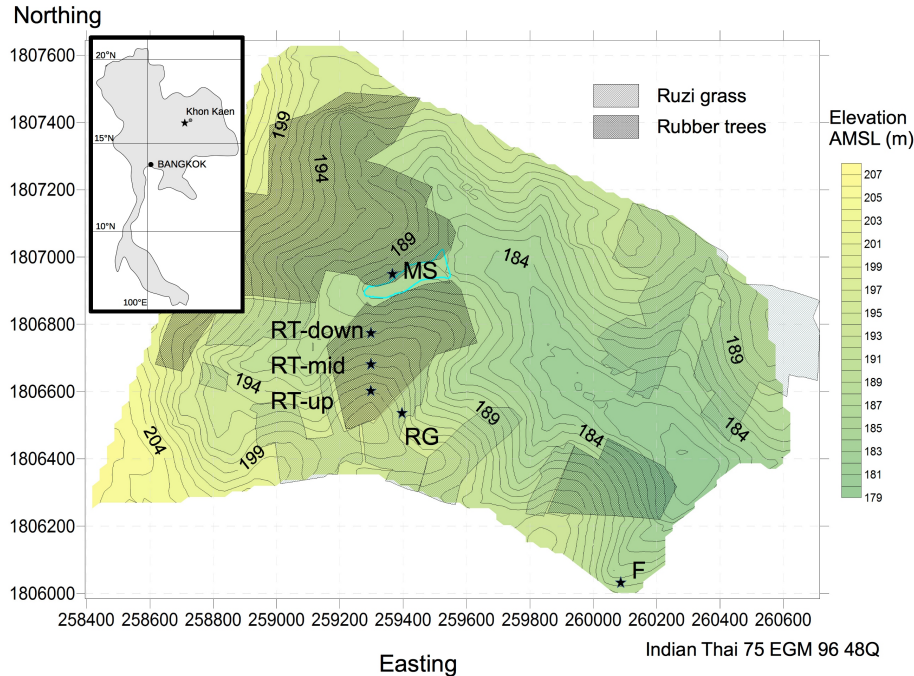
**Figure 1.** Location of the experimental watershed with the different different land uses and measurement sites; F: forest, RG: Ruzi Grass, RT-up: Rubber Tree upslope, RT-mid: Rubber tree mid-slope, RT-down: Rubber Tree downslope, and location of the meteorological station MS.

Title Page

Abstract | Introduction

Conclusions | References

Tables | Figures

|◄ | ►|

◄ | ►

Back | Close

Full Screen / Esc
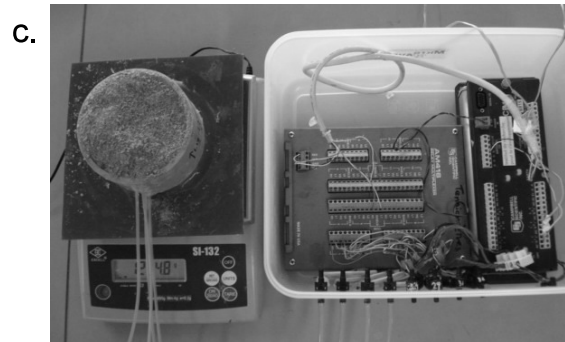
Printer-friendly Version
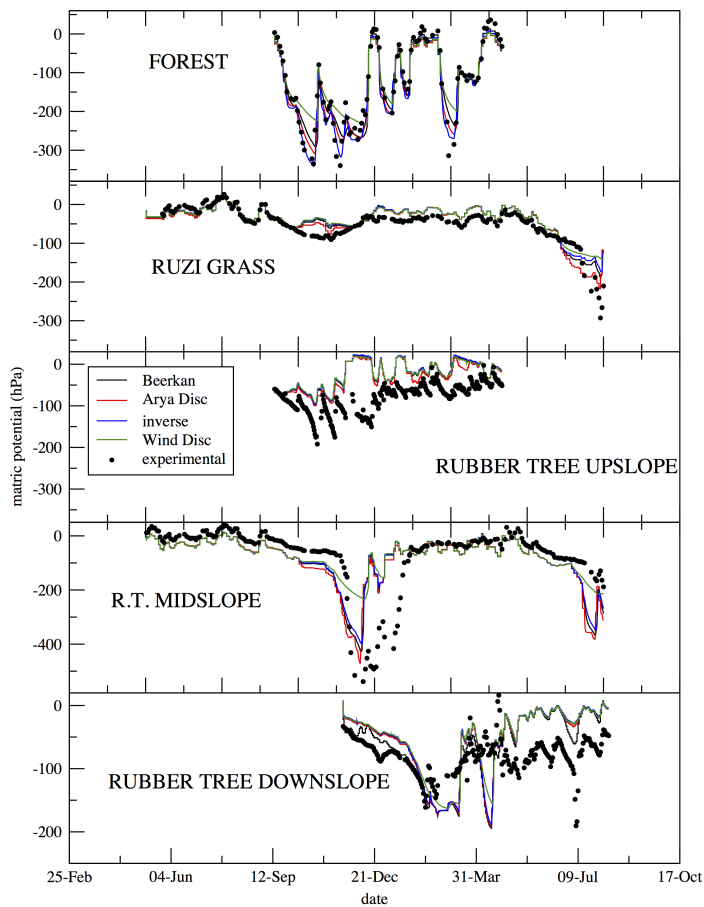
Interactive Discussion

**Estimating unsaturated hydraulic properties**

S. Siltecho et al.

⏮   ⏭

◀   ▶

Back   Close

Full Screen / Esc

Printer-friendly Version

Interactive Discussion

**Figure 2.** Photographs of some of the experimental measurement methods; **(a)** Disc infiltrom-eter; **(b)** Beerkan method; **(c)** Evaporation method.
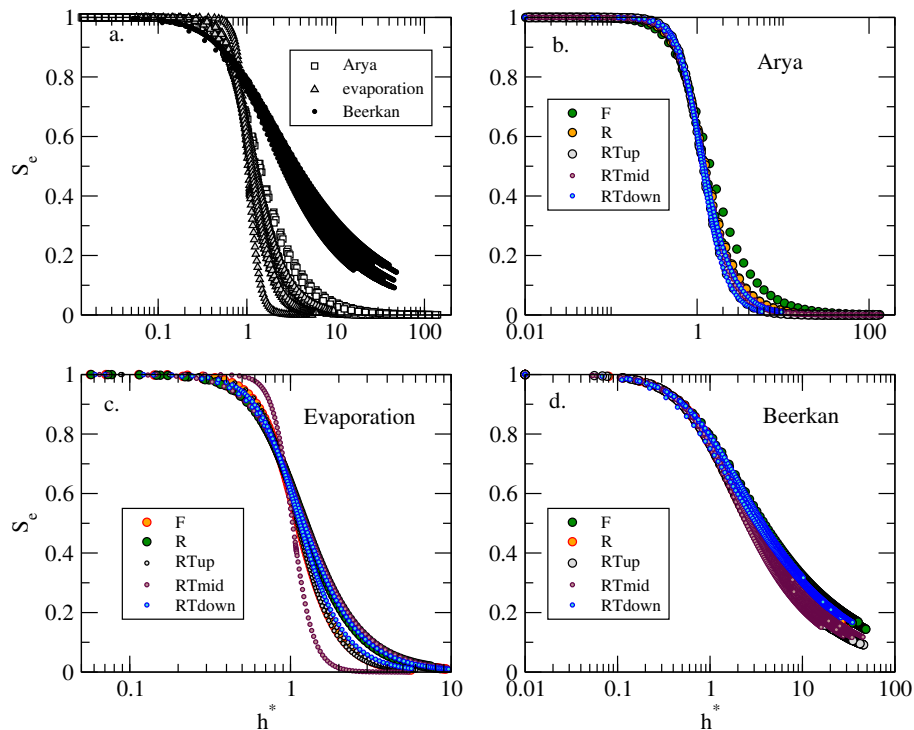
**Figure 3.** Scaled retention curves for **(a)**: the different methods; **(b)**: the method based on Arya's PTF; **(c)**: the evporation method; **(d)**: Beerkan method.

**Figure 4.** Development of the matric potential at 0.25 m depth in the different locations (black dots) and results of modeling with Hydrus1D (continuous lines).
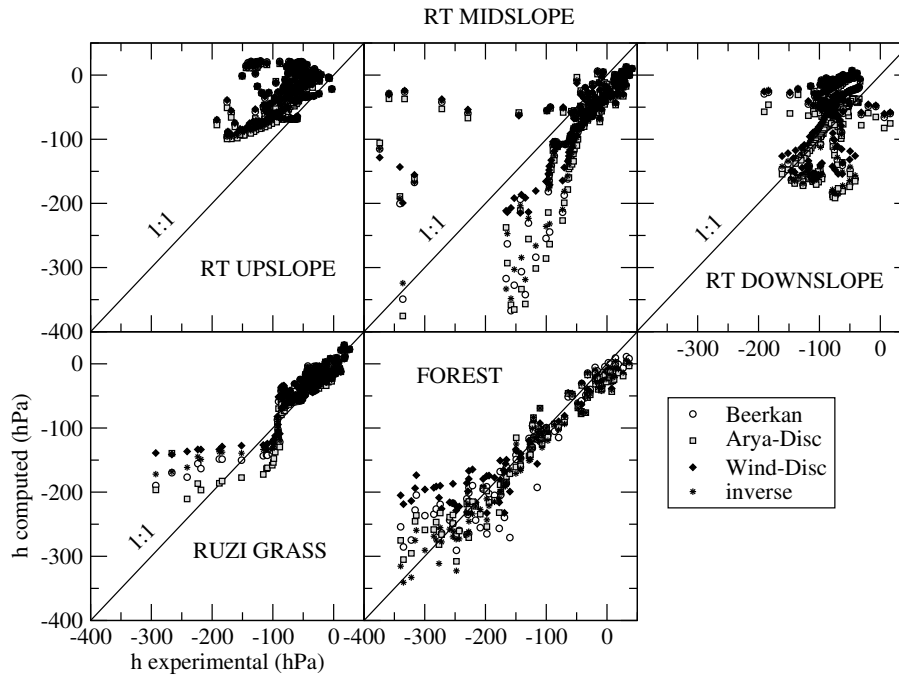
**Figure 5.** Scatter plots of computed vs. experimental matric potential values in the different locations for different combination of parameters.

Title Page

Abstract | Introduction

Conclusions | References

Tables | Figures

|◄ | ►|

◄ | ►

Back | Close

Full Screen / Esc

Printer-friendly Version

Interactive Discussion